JOC The Journal of Organic Chemistry

Article

pubs.acs.org/joc

Application of the Systems Chemistry Approach on the Ammonolysis of 1-Ethoxycarbonyl- and 1-Phenoxycarbonyl-3-(2-thienyl)oxindoles. A Method to Predict Reactivity

Zoltán Mucsi,*[,†,‡] Márta Porcs-Makkay,[§] Gyula, Simig,[§] Imre G. Csizmadia,[†,‡] and Balázs Volk[§]

[†]Department of Chemistry and Chemical Informatics, Faculty of Education, University of Szeged, H-6722 Szeged, Hungary

[‡]Department of Chemistry, University of Toronto, Toronto, Ontario, Canada M5S 3H6

[§]EGIS Pharmaceuticals Plc., Chemical Research Division, P.O. Box 100, H-1475 Budapest, Hungary

Supporting Information

ABSTRACT: The routine prediction of the reactivity of a complex, multifunctional molecule is a challenging and time-consuming procedure. In the last step of the synthesis of the well-known drug substance tenidap, a nonexpected difference was observed between the reactivities of two closely related carbamate moieties, the *N*-ethoxycarbonyl and the *N*-phenoxycarbonyl group. A detailed kinetic study, necessitating a significant computational effort, is described in the present paper for this reaction step. On the other hand, the systems chemistry concept, by analyzing the details of the electronic structure and the connections between functional groups in a fast and simple way, is also able to answer this question using various "-icity" parameters (aromaticity, carbonylicity, olefinicity). The complete systems chemistry approach involves all these conjugativicity parameters, while its further simplified version is based on only one key parameter, which is carbonylicity in the present case. The above methods were compared in terms of their predictive power. The results show that the systems chemistry concept, even its one-parameter version, is applicable for the characterization of this challenging reactivity issue.

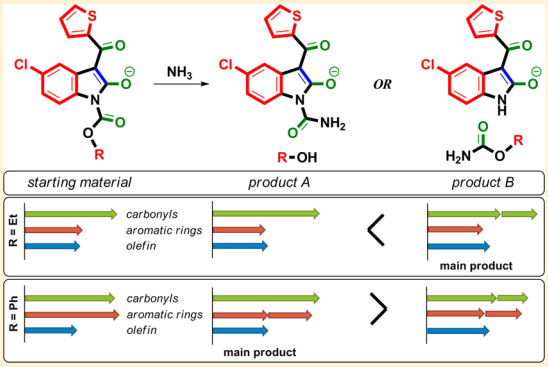

1. INTRODUCTION

In modern organic and medicinal chemistry, a typical molecule may involve several similar functional groups, each of which is able to react with a reagent selectively, resulting in different products. Therefore, the fast determination or at least estimation of the reactivity of these functional groups is essential for planning synthetic routes. Nevertheless, in the case of theoretical methods, which can predict reactivities by modeling the reaction mechanism, it is typical that the real mechanism of a seemingly simple chemical reaction is quite complex, involving many species in each individual elementary step, like reactants, reagents, solvent molecules, catalysts, as well as acid or base as co-reagents.[1−4] All these species should be involved in the calculation in order to investigate the real and detailed mechanism and to get a correct and accurate view of the reaction, which is taking place in a real medium. In fact, determination of the minimal size of the appropriate chemical model (e.g., number of explicit solvent molecules necessary) is very difficult, and it is time and resource consuming.[1] Moreover, an incorrect chemical model provides not only inaccurate energy values, but frequently completely wrong or opposite results, questioning the competence of theoretical methods.[1] Reactions taking place in solution usually require the consideration of a catalyst together with many solvent molecules in an appropriate 3D arrangement.[1,5] Taking into consideration all these factors, it seems nearly impossible to model even a simple acylation reaction.

On the other hand, it was demonstrated earlier that the computation of one or a few, easily and quickly computable, quantum mechanical (QM) descriptors such as aromaticity,[6−9] amidicity,[10−12] carbonylicity,[13] olefinicity,[14,15] and others can predict properly and sometimes even quantitatively certain reactivity and selectivity issues. The global and complex view of these descriptors was defined as conjugativicity in the concept of systems chemistry.[16,17] For example, amidicity percentage is able to predict whether a transamidation reaction takes place under the given conditions or not[10−12] and it can also identify the most reactive amide group of a molecule. It was shown that amide carbonyl groups exhibiting a lower amidicity value were more reactive toward nucleophilic reagents (like amines) than carbonyl groups having a larger amidicity value.[12] Moreover, when more products can be deduced from the reactant it was demonstrated that the difference between the sum of amidicity percentages of products and the sum of those values in the reactants indicated the direction of the transamidation reaction. If this difference is positive, the reaction is energetically favored, while in the case of a negative value the reaction is

Received: April 9, 2012
Published: August 17, 2012

   dx.doi.org/10.1021/jo300715d | J. Org. Chem. 2012, 77, 7282−7290

Scheme 1. Synthesis of tenidap

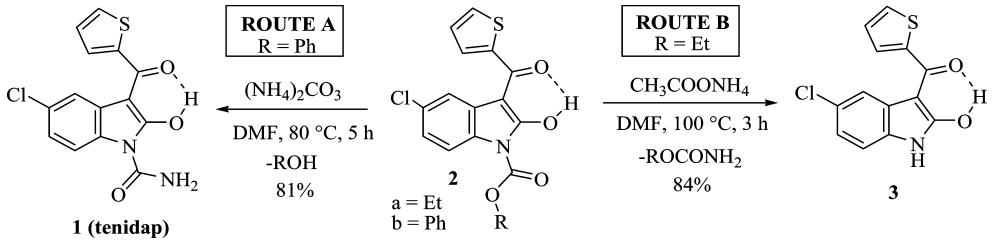

Scheme 2. Neutral and Anionic Structure of Compound 2

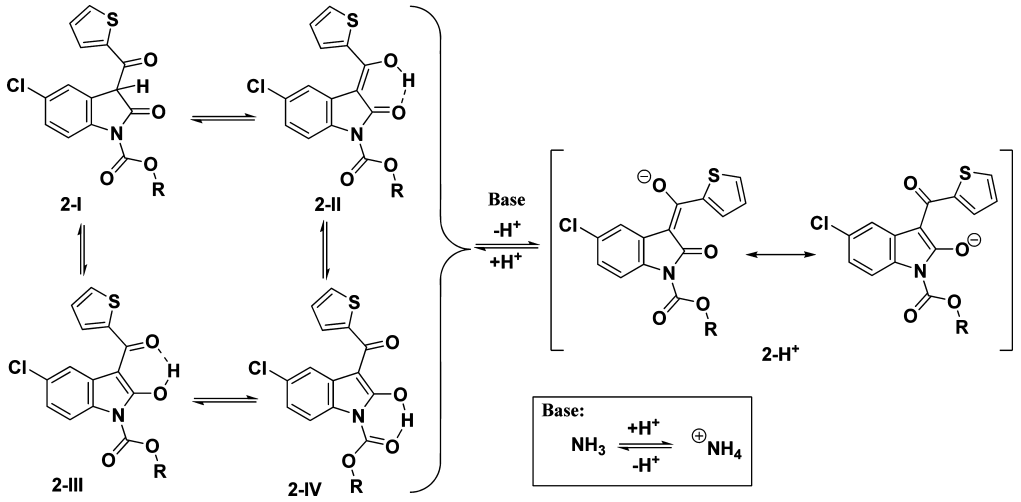

Table 1. Calculated Enthalpy (ΔH) and Gibbs Free Energy (ΔG) in kJ mol^{-1} for 2-I, 2-II, 2-III, 2-IV, and 2-H$^+$ with Et (a) and Ph (b) Substitution in Two Different Solvents (Toluene Is Modeled in Vacuo), Computed at B3LYP/cc-pVTZ Level of Theory, Using the IEF-PCM Method, with Respect to Scheme 2

		2-I		2-II		2-III		2-IV		2-H$^+$	
		Et(a)	Ph(b)	Et(a)	Ph(b)	Et(a)	Ph(b)	Et(a)	Ph(b)	Et(a)	Ph(b)
in vacuo (toluene)	ΔH	30.3	30.1	0.0	0.0	9.9	9.7	39.1	40.6	523.2	517.2
DMF	ΔG	24.2	25.0	0.0	0.0	9.8	10.9	40.2	40.1	522.1	516.1
	ΔH	21.2	21.8	0.0	0.0	12.6	13.6	23.4	24.1	40.6	43.2
	ΔG	15.5	15.4	0.0	0.0	12.9	13.3	23.8	24.8	36.9	39.1

disadvantageous from the driving force point of view. The reaction route for which the sum of amidicity percentages for products is larger than that for other possible reaction routes, is predicted to be the favorable one.[12]

A similar conclusion was drawn for acyl-transfer reactions using carbonylicity as the descriptor.[13] It should be noted, however, that these simple views of a reaction do not consider the kinetic factors, which sometimes perturb the simplest and quickest conclusion. For example, as presented in an earlier work,[13] in the case of acyl-transfer reactions it is not enough to find only the lowest carbonylicity value, but the quitting group should also be a good leaving group.

To demonstrate the efficacy of these precise QM descriptors, an interesting reactivity issue of closely related carbonyl groups is outlined from previous experimental studies on 3-(2-thienyl)oxindoles. In the last step of the synthesis of tenidap (**1**, Scheme 1), reaction of intermediate **2**, depending on the character of the R substituent (Et or Ph), can lead to different products (**1** or **3**).[18] Stirring of **2b** in DMF at 75−80 °C for 5 h with ammonium carbonate resulted in the formation of compound **1** in 81% yield,[18] while in the case of ethyl ester **2a**, simply the ammonium salt of **2a** was isolated under these conditions. Application of an other ammonia source (ammonium acetate) and more vigorous reaction conditions (DMF, 100 °C, 3 h) for the ammonolysis of **2a** resulted in the formation of the deethoxycarbonylated product **3** in 84% yield.

2. RESULTS AND DISCUSSION

2.1. Kinetic Study Involving Tautomeric, Conformational and Protonation Pre-equilibria. In general, 1-alkoxy(aryloxy)carbonyl-3-(2-thienyl)oxindoles exist in three tautomeric forms (**2-I**, **2-II**, and **2-III**, Scheme 2) and an additional rotamer of **2-III**, coded as **2-IV**, where R may be equal to either Et or Ph substitution. According to the computational results (Table 1), **2-II** is the most stable form both in vacuo and in DMF,for both the Et and Ph substitution. Single-crystal X-ray measurement supports this computational result: compound **2** exhibits geometry **2-II** also in the solid state.[18] In solution, under basic conditions, compound **2** can be deprotonated, resulting in **2-H**$^+$, which can be represented in one form, but with two main contributing resonance structures (Scheme 2).

dx.doi.org/10.1021/jo300715d | J. Org. Chem. 2012, 77, 7282−7290

Scheme 3. Proposed Mechanism for the Transformation of 2, Starting from the Anionic Form Reactant

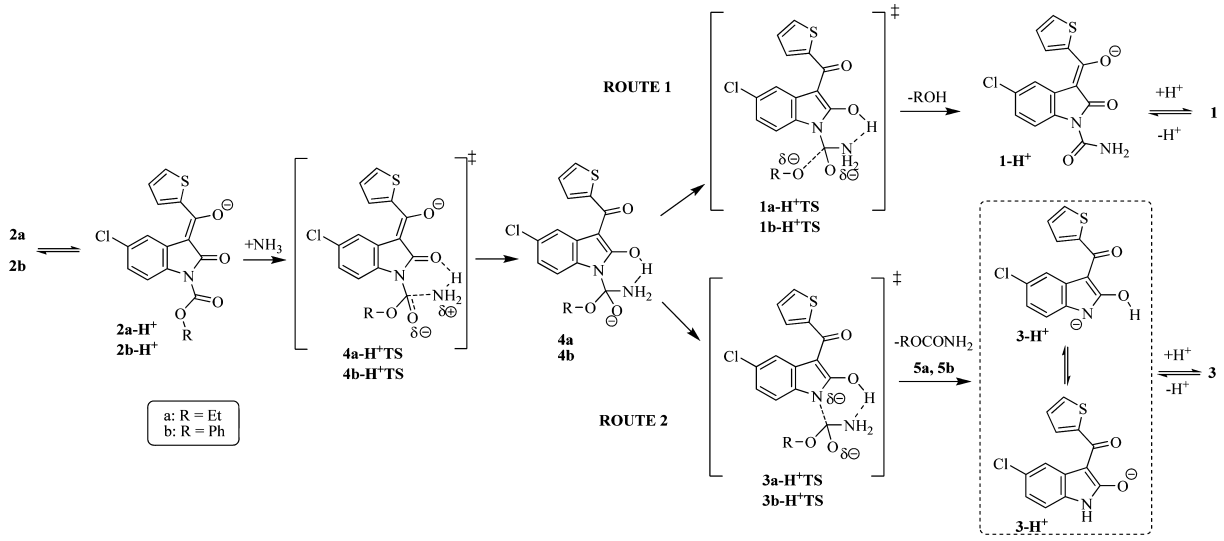

Coming back to the difference in reactivity between **2a** and **2b** toward NH_3 under ammonolysis conditions (Scheme 1), the suggested mechanism starts with a deprotonation−protonation equilibrium between **2** and **2-H$^+$**. Among the three carbonyl groups, the carbonyls *C*(2)═O and *C*(3)−COAr can be ignored from the mechanistic study due to the nonexisting reaction pathway since no TSs and intermediates were identified. In agreement with the experimental study, the only reactive carbonyl moiety of **2-H$^+$** is at the *N*(1) atom. Starting from **2** (Scheme 3), the first step (**2** → **4-H$^+$TS**) is the addition of the NH_3 species to the carbonyl group at *N*(1), requiring a +154.4 and +144.9 kJ mol^{-1} activation Gibbs free energy ($\Delta G^{\ddagger}$) for R = Et (**2a-H$^+$**) and R = Ph (**2b-H$^+$**), respectively (Figure 1, Table 2) in DMF medium. After the TS (**4-H$^+$TS**), a high energy intermediate (**4**) is formed, where the H atom from the NH_3 moves to the negatively charged carbonyl oxygen of the indole ring. From this point, the mechanism is branched into two routes (routes 1 and 2), leading to the two possible products (**1** and **3**) through two low energy TSs (**1-H$^+$TS** and **3-H$^+$TS**) after proton exchange with the leaving groups.

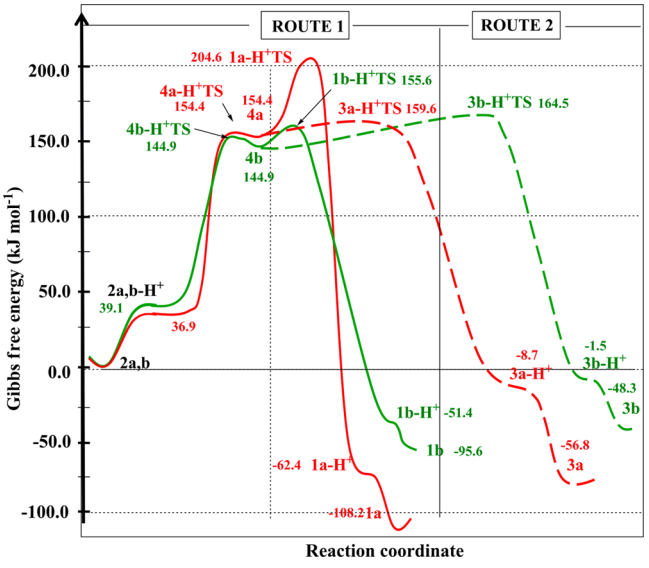

Figure 1. Gibbs free energy reaction profile of the transformations **2** → **1** and **2** → **3**, computed at B3LYP/cc-pVTZ level of theory, using IEF-PCM method.

Table 2. Enthalpy (ΔH, in kJ mol^{-1}) and Gibbs Free Energy (ΔG, in kJ mol^{-1}) for the Transformation of 2 to 1 and 3, Computed at B3LYP/cc-pVTZ Level of Theory, Using IEF-PCM Method in DMF

	R = Et(a)		R = P (b)	
	H	*G*	*H*	*G*
protonation preequilibrium				
2-I + NH_3 → 2-H$^+$ + NH_4^+ (in DMF)	0.0	**0.0**	0.0	**0.0**
rate-determining step				
2-H$^+$ + NH_3	40.6	**36.9**	43.2	**39.1**
2-H$^+$ + NH_3 → 4-H$^+$TS	109.6	**157.1**	100.81	**154.37**
2-H$^+$ + NH_3 → **4**	109.0	**154.4**	97.87	**144.87**
route 1				
4 → 1-H$^+$TS	53.1	**50.2**	13.1	**10.7**
4 → 1-H$^+$ + ROH	−214.9	**−216.8**	−193.1	**−196.3**
1-H$^+$ → **1**	−212.7	**−262.6**	−189.5	**−240.5**
route 2				
4 → 3-H$^+$TS	6.2	**5.2**	24.1	**19.6**
4 → 3-H$^+$ + **5**	−160.6	**−163.1**	−142.9	**−146.4**
3-H$^+$ → **3**	−161.6	**−211.2**	−141.7	**−193.2**

For R = Et, the oxindole anion (**3-H$^+$**) in route 2 proved to be a better leaving group than the EtO^- in route 1; therefore, **3-H$^+$** and $EtOCONH_2$ (**5a**) form as products, instead of **1-H$^+$** and EtOH. The Gibbs free energy level of **3a-H$^+$TS** is lower by 45.0 kJ mol^{-1} than that of **1a-H$^+$TS**, which allows exclusively route 2 (Figure 1, Table 2).

The opposite case can be concluded for R = Ph, where the leaving of PhO^- anion is more advantageous than the leaving of the oxindole anion (**3-H$^+$**), due to the lower TS energy for route 1 (**1b-H$^+$TS**) than for route 2 (**3b-H$^+$TS**). In this case, therefore, **1-H$^+$** and PhOH appear as products. The Gibbs free energy level of **1b-H$^+$TS** is lower by 8.9 kJ mol^{-1} than that of **3b-H$^+$TS** (Figure 1, Table 2). It should be mentioned, however, that the formation of **1b-H$^+$** is thermodynamically more advantageous than the formation of **3b-H$^+$**; therefore, the formation of **3b-H$^+$** together with **3b** is only kinetically preferred because of the lower energy TS in DMF medium.

dx.doi.org/10.1021/jo300715d | J. Org. Chem. 2012, 77, 7282−7290

Scheme 4. Proposed Mechanism for the Transformation of 2, Starting from the Neutral Reactant

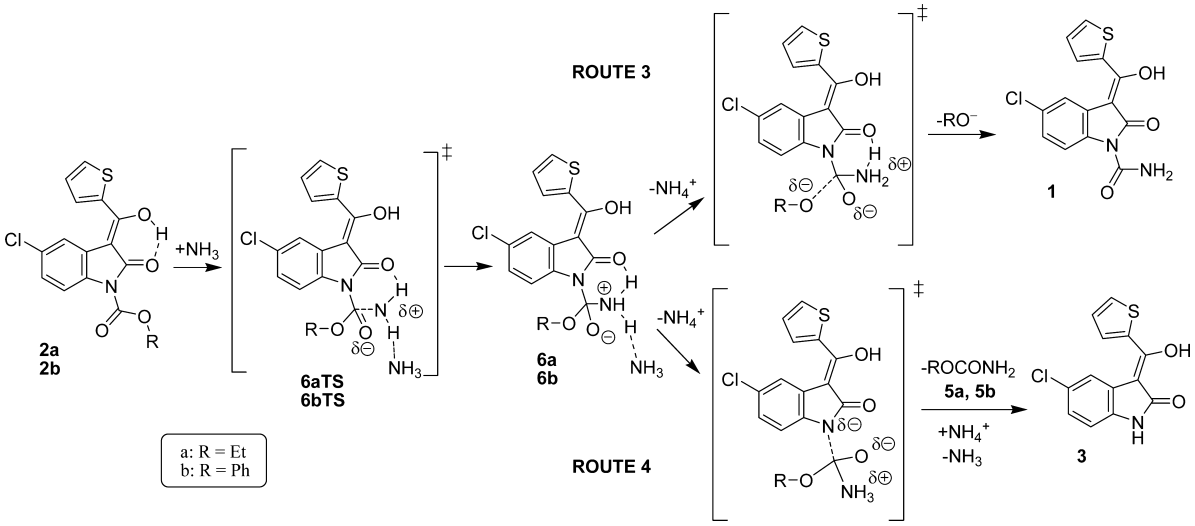

Scheme 5. Summary of the Systems Chemistry Analysis of the Transformation of 2-H$^+$ via Route 1, Yielding 1-H$^+$ and RO$^-$ and via Route 2, Providing 2-H$^+$ and 5, Computed at the B3LYP/cc-pVTZ Level of Theory, Using the IEF-PCM Method[a]

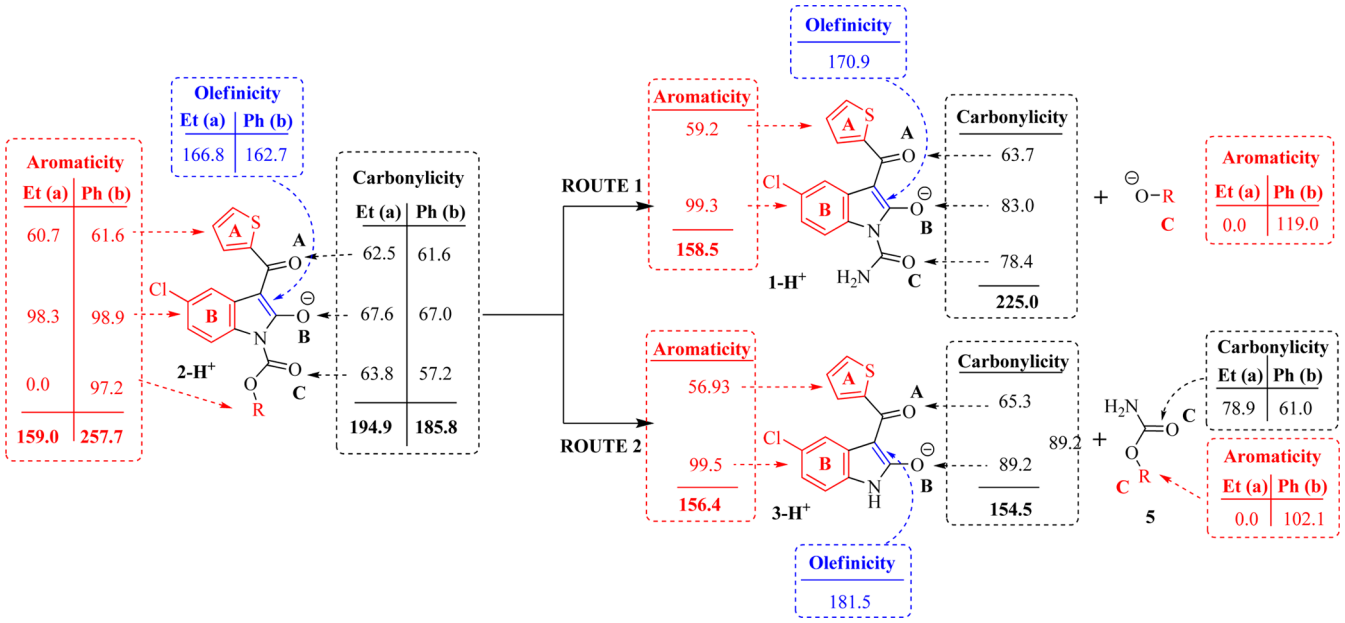

[a]Aromaticity, olefinicity, and carbonylicity values in percent. Red color represents the aromatic functionalities with their aromaticity values in percent; blue bonds show the olefinic moieties in the indole ring, together with their olefinicity values in percent. The remaining black parts indicate the carbonyl functionalities together with their carbonylicity values in percent.

It should be mentioned that an alternative mechanism (depicted in Scheme 4) starting from the neutral **2** was also investigated and proved to be not feasible to produce the expected products because the indolinone carbonyl group is not able to get the proton from the attacking NH_3. Consequently, intermediate **6** did not prove to be a real minimum nor **6TS** is a real TS. Involving additional ammonia as a proton transfer agent of this reaction did not help the reaction to proceed.

2.2. Complete Systems Chemistry Analysis. From the systems chemistry point of view, all of the chemical components taking part in the reaction can be described with three components, carbonylicity, aromaticity, and olefinicity.[14,15] The chemical system of **2-H$^+$** can be represented by one olefinic bond (Scheme 5, Figure 2, blue bond), three carbonyl groups (black bonds), as well as two aromatic rings in **2a-H$^+$** and three in **2b-H$^+$** (red functionalities). The two main products **1-H$^+$** and **3-H$^+$** are analogously composed of also one olefinic bond, two carbonyl groups (black bonds), and two aromatic rings. The side product PhO^- has one aromatic ring; **5a** involves one carbonyl group, while **5b** involves one carbonyl moiety and an aromatic ring. Finally, EtO^- has no conjugative functional groups from this aspect. According to this calculation, one can analyze the small energy changes from the starting state to the product state, when the percentage values are recalculated into their energy values (see section 4.2, eqs 3, 5, and 7). The corresponding resonance energies are illustrated by arrows in Figure 2 by keeping the definition of the colors. Sums of the corresponding aromaticities and olefinicity

dx.doi.org/10.1021/jo300715d | J. Org. Chem. 2012, 77, 7282−7290

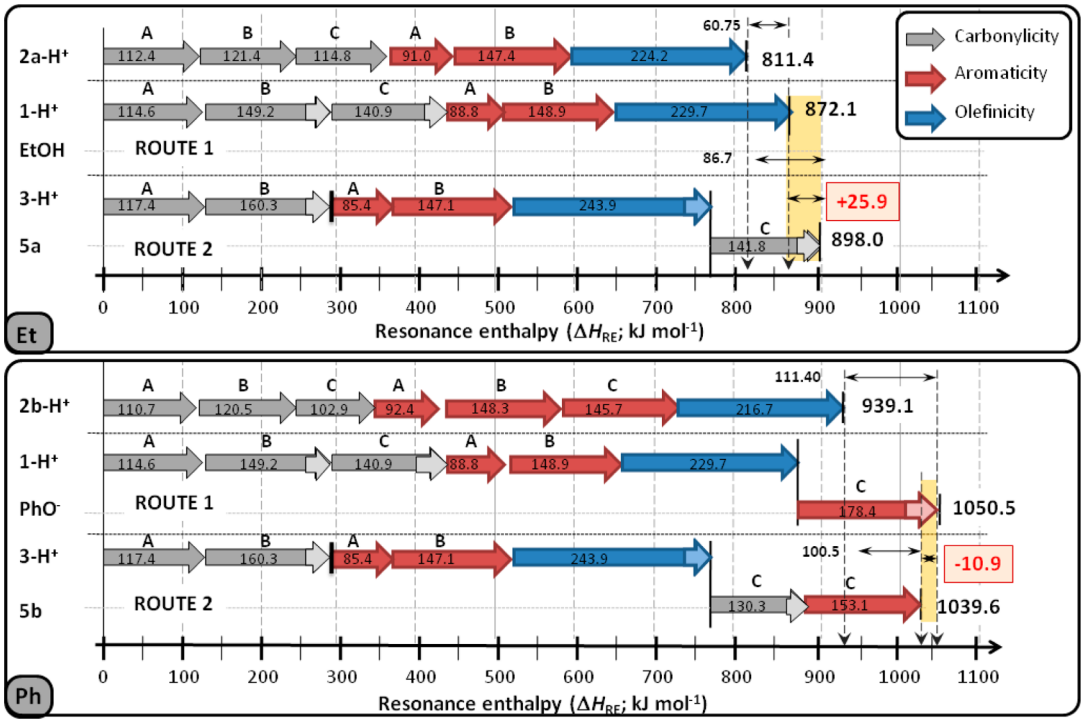

Figure 2. Systems chemistry analysis for the reaction of **2a-H$^+$** and **2b-H$^+$** via Routes 1 and 2, computed at the B3LYP/cc-pVTZ level of theory, using IEF-PCM method. The light colors at the end of the arrows indicate the increase with respect to the starting material **2-H$^+$**.

Table 3. Complete Systems Chemistry Analysis for the Reaction of 2a-H$^+$ via Routes 1 and 2, Computed at the B3LYP/cc-pVTZ Level of Theory, Using the IEF-PCM Method

	conjugativicity					
compd	type[a]	%	ΔH_{RE} (kJ mol^{-1})	Σ1 (kJ mol^{-1})	Σ2 (kJ mol^{-1})	Σ3 (kJ mol^{-1})
			reactant			
2a-H$^+$	CA	62.5 + 67.6 + 63.8	112.4 + 121.6 + 114.8	348.8	811.4	**811.4**
	AR	60.7 + 98.3	91.0 + 147.4	238.4		
	OL	166.8	224.2	224.2		
			products (route 1)			
1-H$^+$	CA	63.7 + 83.0 + 78.4	114.6 + 149.2 + 140.9	404.8	872.1	**872.1**
	AR	59.2 + 99.3	77.7 + 143.7	237.7		
	OL	170.9	229.7	229.7		
EtOH				0.0	0.0	
			products (route 2)			
3-H$^+$	CA	65.3 + 89.2 + 0.0	117.4 + 160.3 + 0.0	277.8	756.2	**989.0**
	AR	56.9 + 99.5	85.4 + 149.2	234.6		
	OL	181.5	243.9	243.9		
5a	CA	78.9	141.8	141.8	141.8	

[a]CA = carbonylicity; AR = aromaticity; OL = olefinicity.

and carbonylicity resonance energies of the starting state **2-H$^+$**, as well as for the two product states **1-H$^+$** + RO$^-$ (route 1) and **3-H$^+$** + **5** (route 2), are summarized in Figure 2 and Tables 3 and 4. In all cases, the overall resonance energies of the two product states are larger than those of the starting states, therefore all reaction routes are rational from the energetical aspect.

In the case of Et substitution (**a**), route 2 exhibits a large overall resonance enthalpy for **3a-H$^+$** + **5a** (898.0 kJ mol^{-1}), by 25.9 kJ mol^{-1} higher than route 1 for **1a-H$^+$** (872.1 kJ mol^{-1}), predicting route 2 to be the dominant mechanism. The opposite result can be obtained for the Ph substitution, where the sum of the corresponding resonance enthalpies of route 1 (1050.5 kJ mol^{-1}) is moderately (by 10.9 kJ mol^{-1}) larger than the analogous value for route 2 (1039.6 kJ mol^{-1}).

One can analyze the molecular details and study the interaction between functional groups. In the case of ethyl substitution, in the course of route 1 (Scheme 5, **2a-H$^+$** → **1-H$^+$**) only the carbonylicity value of the carbonyl moieties B and C of **2a-H$^+$** increased in the product **1-H$^+$**, in addition to negligible changes of carbonyl A, aromatic rings A and B, and the olefinic bond. The overall resonance enthalpy difference ($\Sigma\Delta H_{RE}$) between the product state **1-H$^+$** + **EtOH** and the starting state **2a-H$^+$** is 60.8 kJ mol^{-1}. With the same substitution, in the course of route 2 [**2a-H$^+$** → **3-H$^+$**], analogously to the above, carbonylicity of moieties B and C increased significantly, but here the change in the olefinicity

dx.doi.org/10.1021/jo300715d | J. Org. Chem. 2012, 77, 7282−7290

Table 4. Complete Systems Chemistry Analysis for the Reaction of 2b-H$^+$ via Routes 1 and 2, Computed at the B3LYP/cc-pVTZ Level of Theory, Using the IEF-PCM Method

	conjugativicity					
compd	type[a]	%	ΔH_{RE} (kJ mol^{-1})	Σ1 (kJ mol^{-1})	Σ2 (kJ mol^{-1})	Σ3 (kJ mol^{-1})
			reactant			
2b-H$^+$	CA	61.6 + 67.0 + 57.2	110.7 + 120.5 + 102.9	334.1	939.1	**939.1**
	AR	61.6 + 98.9 + 97.2	92.4 + 148.3 + 145.7	386.4		
	OL	162.7	218.7	218.7		
			products (route 1)			
1-H$^+$	CA	63.7 + 83.0 + 78.4	114.6 + 149.2 + 140.9	404.8	872.1	**1050.5**
	AR	59.2 + 99.3	88.8 + 148.9	237.6		
	OL	170.9	229.7	229.7		
PhO$^-$	AR	119.0	178.4	178.4	178.4	
products (route 2)						
3-H$^+$	CA	65.3 + 89.2 + 0.0	117.4 + 160.3 + 0.0	277.8	756.2	**1039.6**
	AR	56.9 + 99.5	85.4 + 149.2	234.5		
	OL	181.5	243.9	243.9		
5b	CA	61.0	130.3	130.3	283.5	
	AR	102.2	153.2	153.2		

[a]CA = carbonylicity; AR = aromaticity; OL = olefinicity.

Table 5. Calculated Carbonylicity Percentages of Compounds 2-H$^+$, 1-H$^+$ and 3-H$^+$, Computed at the B3LYP/cc-pVTZ Level of Theory, Using the IEF-PCM Method

	R = Et (a); CA %				R = Ph (b); CA %			
compd	A or A′	B	C	Σ	A or A′	B	C	Σ
2-H$^+$	63.8	67.6	62.5	**193.9**	61.6	67.0	57.2	**185.8**
				route 1				
1-H$^+$	63.7	83.0	78.4	**225.1**	63.7	83.0	78.4	**225.1**
				route 2				
3-H$^+$	65.3	89.2	**154.5**	65.3	89.2			**154.5**
5			78.9	**78.9**			61.0	**61.0**
sum				**233.4**				**215.4**

value is also positive, due to the larger aromaticity of the oxindole ring in product **3-H$^+$**. Here the $\Sigma\Delta H_{RE}$ difference is significantly larger (86.6 kJ mol^{-1}). The sum of carbonylicity values of moieties A, B, and C is somewhat larger in **3-H$^+$** than in **1-H$^+$**, but the most characteristic difference between routes 1 and 2 can be identified as the increase of the olefinicity value in favor of product **3-H$^+$**, referring to a more aromatic indole ring in the case of this product. The lower aromaticity of the indole ring in product **1-H$^+$** can be explained by the competitive delocalization of the lone electron pair of the nitrogen atom between the indole aromatic ring and carbonyl group C.

In the case of phenyl substitution, the changes in resonance energies in the case of route 2 are close to those of the ethyl-substituted analogue: the $\Sigma\Delta H_{RE}$ value between the product state **3-H$^+$** + **5b** and the starting state **2b-H$^+$** is 86.6 kJ mol^{-1}, practically the same as the one calculated for ethyl substitution. Very similar changes can be observed in the course of the two mechanisms. On the other hand, a sharp difference can be observed in the aromaticity of the aromatic ring C in route 1: the phenyl ester group with a common aromaticity value (97.2%) is leaving as PhO$^-$ anion, which exhibits a very large aromaticity value (119.0%). It increases the overall $\Sigma\Delta H_{RE}$ to 111.4 kJ mol^{-1} and finally makes this route 1 the favored mechanism because of the net H_{RE} benefit of 10.9 kJ mol^{-1}.

2.3. One-Parameter Systems Chemistry Analysis: Carbonylicity as the Driving Force of Ammonolysis. Although the complete systems chemistry approach represents a significant simplification in the determination of the reaction pathway when compared to the detailed kinetic study, it still necessitates a considerable amount of work, as outlined in the previous section. It may raise the question whether there is an even simpler and faster method to answer such a question. For this reason, a one-parameter systems chemistry approach was applied to this two-step reaction. In the first step, the most reactive carbonyl group of the two starting materials (**2a-H$^+$**, **2b-H$^+$**) needs to be found, and in the second step, the product to be formed should be predicted.

When calculating the carbonylicity values of the three different carbonyl groups (**A**, **B**, **C**, see Scheme 5), one may conclude that the oxindole carbonyl group (**B**) exhibits the largest values, irrespectively to the R substituents [67.6% for Et (**a**); 67.0% for Ph (**b**)], referring to the most resistant carbonyl group against nucleophilic attack. The lowest value was obtained for the carbonyl moiety **C** [62.5% for Et (**a**); 57.5% for Ph (**b**)], indicating the most reactive position of the molecule against nucleophilic attack. The second lowest values were computed for carbonyl moiety **A** (63.8% and 61.6%), supposing a less reactive carbonyl, but here the thiophene group is not a real leaving group; thus, its elimination from the molecule would require a high activation energy, which makes this reaction path kinetically unfavored (Scheme 5).

In the cases of both R substituents [Et (**a**) and Ph (**b**)] and for both reaction routes (routes 1 and 2, Scheme 5 and Table 5), the sum of the carbonylicity percentages of the corresponding primary products (**1-H$^+$** and **3-H$^+$** + **5**) are larger than that in the corresponding reactant (**2-H$^+$**),

dx.doi.org/10.1021/jo300715d | J. Org. Chem. 2012, 77, 7282−7290

predicting an energetically favored ammonolysis process. This is in good correlation with results of the previous paragraphs, predicting an exothermic reaction. According to the calculated carbonylicity percentages, in the case of ethyl substitution (**2a-H**$^+$), route 2 is predicted to be more favorable due to the larger value of the sum of the three carbonylicity percentages for product **1-H**$^+$, compared to the sum of the three carbonylicity percentages for products **3-H**$^+$ and **5a** via route 1 (Table 5). However, opposite results can be predicted for the R = Ph case, where the sum of the carbonylicity percentages for products **3-H**$^+$ and **5b** is larger than for route 2 (Scheme 5, Table 5).

The one-parameter systems chemistry method alone was also able to answer this reactivity issue; however, the calculated differences in carbonylicity percentages are not as significant as in the multiparameter method. Although the main characteristic of this reaction is the acyl transfer, but in a full picture, other additional changes in aromaticity and olefinicity also take part in the process, making a significant overtone to the overall reaction. The consideration of the whole system allows a better established conclusion, but the determination of the characteristic changes during the reaction, like carbonylicity in the present case, is faster and is sufficient for the prediction of the favorable reaction pathway.

In Table 6, the computational demand of the traditional methods, where the real reaction mechanism is explored, is compared with the application of systems chemistry. In the traditional method, many possible routes have to be investigated, including some crucial participants (catalyst, solvent, etc.). In this particular case, the finally selected mechanism requires nearly the same number of optimized geometries as the systems chemistry method. Nevertheless, to that number one needs to add the number of optimized TSs, which necessitate significantly more time-consuming computations than a normal geometry optimization. When comparing the total computational background, the high efficacy of systems chemistry is well demonstrated.

Table 6. Comparison of the Traditional and Systems Chemistry Method To Predict the Product Selectivity of the Reactions Studied[a]

	kinetic study		one-parameter systems chemistry
	overall comp work	comp work for selected mechanism	comp work for carbonylicity value
optimization	>80	16	17
TS optimization	>20	6	0

[a]The numbers in the table represent optimized geometries.

3. CONCLUSION

In the present paper, the mechanism of ammonolysis of 1-ethoxycarbonyl- and 1-phenoxycarbonyl-3-(2-thienyl)oxindoles is discussed. It has been demonstrated that a new theoretical method called systems chemistry could predict and the different reactivity of the closely related carbamate moieties in this amidation reaction by using a simple computational protocol, without mapping the overall and detailed mechanism by large computational efforts. This procedure clearly shows that systems chemistry, with relatively few computations, can effectively predict reaction mechanism even when keen selectivity issues are present.

4. METHODS

4.1. Experimental Section. *5-Chloro-3-[1-hydroxy-1-(2-thienyl)methylene]-1,3-dihydro-2H-indol-2-one-1-carboxamide (tenidap, **1**). According to Scheme 1, Route A.* To a solution of **2b** (39.8 g, 0.10 mol) in DMF (250 mL) was added ammonium carbonate (15.6 g, NH_3 content 22%, 0.20 mol). The mixture was stirred at 80 °C for 5 h and then was poured into a mixture of ice−water (500 g) and concentrated HCl (25 mL). After the mixture was stirred for an additional 2 h at 0−5 °C, the crystalline product was filtered to give the crude tenidap (**1**, 32.3 g, ca. 100%) as yellow crystals, mp 221−224 °C. The crude product was purified as follows: it was dissolved in a refluxing mixture of methanol (635 mL) and 2-aminoethanol (6.30 mL, 6.40 g, 0.11 mol) and treated with charcoal (1 g). After filtration, concentrated HCl (18.8 mL) was added dropwise at 40−45 °C. The suspension obtained was stirred for 2 h at 20−30 °C and filtered to give the title compound (25.8 g, 81%) as yellow crystals, mp 229−230 °C. Characterization of **1** was performed using IR and ^{1}H NMR spectra, identical to those described in ref 18. Anal. Calcd for $C_{14}H_9ClN_2O_3S$: C, 52.42; H, 2.83; Cl, 11.05; N, 8.73; S, 10.00. Found: C, 52.80; H, 2.90; Cl, 10.99; N, 8.59; S, 9.90.

Ammonium Salt of 5-Chloro-1-ethoxycarbonyl-3-[1-hydroxy-1-(2-thienyl)methylene]- 1,3-dihydro-2H-indol-2-one. To a solution of **2a** (0.70 g, 2.0 mmol) in DMF (4 mL) was added ammonium carbonate (0.16 g, NH_3 content 22%, 2.0 mmol), and the mixture was stirred for 5 h at 80 °C. The mixture was cooled to ambient temperature, and water (10 mL) was added. The solid precipitate was filtered to give the ammonium salt of **2a** (0.61 g, 83%) as yellow crystals, mp 192−194 °C (lit.[18] mp 193−197 °C). Characterization of the product was performed using IR and ^{1}H NMR spectra, identical to those described in ref 18. Anal. Calcd for $C_{16}H_{15}ClN_2O_4S$: C, 52.39; H, 4.12; Cl, 9.67; N, 7.64; S, 8.74. Found: C, 52.33; H, 4.08; Cl, 9.85; N, 7.38; S, 8.65.

*5-Chloro-3-[1-hydroxy-1-(2-thienyl)methylene]-1,3-dihydro-2H-indol-2-one (**3**). According to Scheme 1, Route B.* To a solution of **2a** (3.50 g, 10 mmol) in DMF (25 mL) was added ammonium acetate (1.50 g, 20 mmol). The mixture was stirred at 100 °C for 3 h and then poured into a mixture of ice−water (50 g) and concentrated HCl (2.5 mL). The mixture was stirred for additional 2 h at 0−5 °C, and the crystalline product was filtered to give **3** (2.33 g, 84%). Characterization of **3** was performed using IR and ^{1}H NMR spectra, identical to those described in ref 21. Anal. Calcd for $C_{13}H_8ClNO_2S$: C, 56.22; H, 2.90; Cl, 12.77; N, 5.04; S, 11.54. Found: C, 56.14; H, 3.03; Cl, 12.65; N, 5.33; S, 11.64.

4.2. Computational Methods. All computations were carried out using the Gaussian03 program package (G03).[19] Geometry optimizations and subsequent frequency analyses were carried out on selected amide-containing systems from which the values for the enthalpy of hydrogenation (ΔH_{H2}) were extracted. Computations were carried out at B3LYP/6-31G(d,p) and B3LYP/cc-pVTZ level of theories.[20] Method and basis sets were chosen for their reliability in the characterization of carbonylicity, in agreement with works published previously.[1,5,13] The vibrational frequencies were computed at the same levels of theory as those used for geometry optimization, in order to properly confirm all structures as residing at minima on their potential energy hypersurfaces (PESs). Thermodynamic functions *U*, *H*, *G*, and *S* (listed in the Supporting Information, Tables S1−S2) were computed at 298.15 K, using

dx.doi.org/10.1021/jo300715d | J. Org. Chem. 2012, 77, 7282−7290

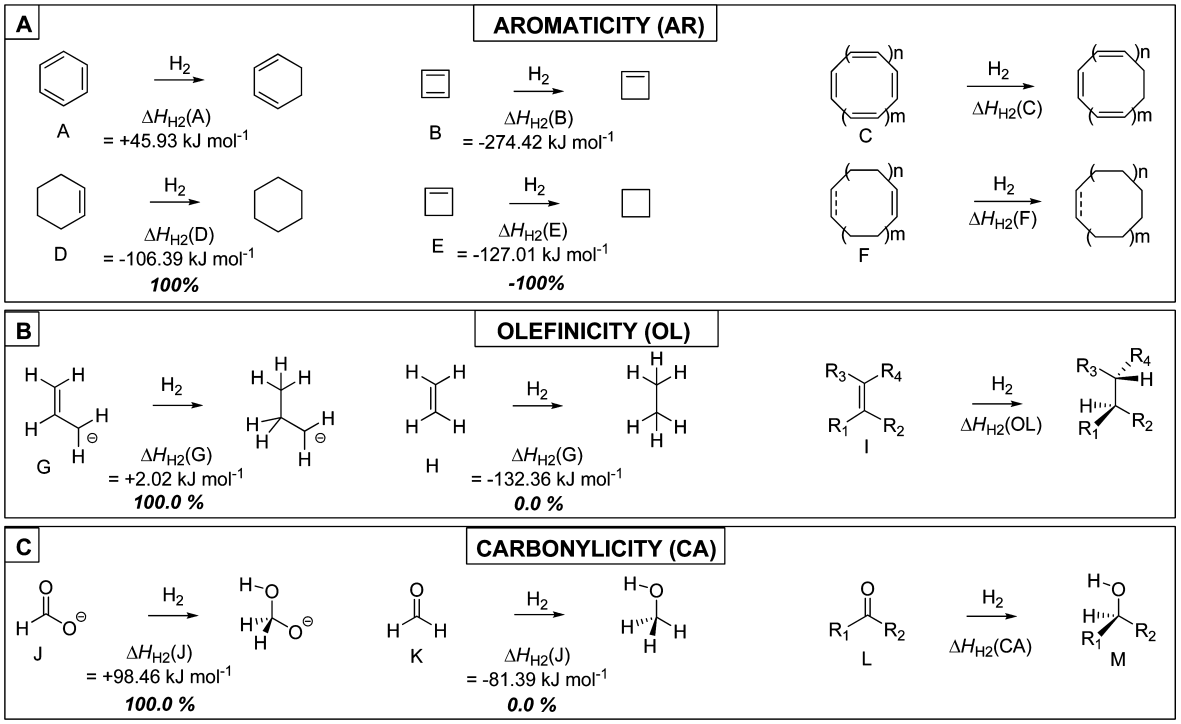

Figure 3. Definition of "-icity" parameters. Values were obtained from the B3LYP/cc-pVTZ geometry-optimized structures. (A) ΔH_{H2} vales calculated for an antiaromatic and aromatic species. (B) The definition of the olefinicity percentage (OL%) based on the enthalpy of hydrogenation (ΔH_{H2}) of the double bond. (C) The definition of the carbonylicity percentages (CA%) is based on the enthalpy of hydrogenation (ΔH_{H2}) of the carbonyl group. In **M**, the H−O−C−X (X = R_1 or R_2) dihedral angles are forced into the *anti* orientation.

the quantum chemical rather than the conventional, thermodynamic reference state. To model the DMF solution, the IEF-PCM (integral equation formalism polarizable continuum medium) method was applied. Due to the convergence problem of reactant−reagent−catalyst complexes, in the case of the solvent model only single point calculations were carried out, considering thermodynamic functions from the frequency calculation in vacuo. According to our estimation, the error of this solvent model was around 1−2 kJ mol^{-1}.

4.3. Stabilization Energy (SE) Protocols. From a systems chemistry point of view, most of the organic chemical structures can be separated into various functional groups as basic characteristics, which are linked together by the global electronic structure of the molecule (Figure 3). These various basic characteristics can easily be described by the concept of conjugativicity, in the present case by aromaticity (AR%),[6−9] olefinicity (OL%),[14,15] and carbonylicity (CA%)[13] percentages at the B3LYP/cc-pVTZ level of theory, using the IEF-PCM method.

Aromaticity Percentage and Its Resonance Enthalpy (AR %). Aromaticity and antiaromaticity[6−9] are characterized by a common and universal linear scale based on the heat of hydrogenation (ΔH_{H2}, Figure 3A), where benzene (**A**) and cyclobutadiene (**B**) are considered as +100% and −100%, respectively. This methodology compares the hydrogenation reaction of the examined compound [**C**, ΔH_{H2}(C)] with that of a properly chosen reference reaction [**F**, ΔH_{H2}(F)]. The difference between the two enthalpy values [$\Delta\Delta H_{H2}$(AR); eq 1] is transformed to aromaticity percentage (AR%; eq 2), including m_{AR} and b_{AR} as linear parameters, which are the basis of the calculation of the resonance enthalpy [H_{RE}(AR); eq 3].

$$\Delta\Delta H_{H2}(\mathrm{AR}) = \Delta H_{H2}(\mathrm{C}) - \Delta H_{H2}(\mathrm{F}) \quad (1)$$

$$\mathrm{AR\%} = m_{AR}\Delta\Delta H_{H2}(\mathrm{AR}) + b_{AR} \quad (2)$$

$$H_{RE}(\mathrm{AR}) = \mathrm{AR\%}/m_{AR} \quad (3)$$

Here, m_{AR} = 0.6670; b_{AR} = 2.5440 at B3LYP/cc-pVTZ in DMF.

Olefinicity Percentage and Its Resonance Enthalpy (OL%). The "olefinicity scale", quantifying alkene bond strength on a linear scale,[14,15] based on the computed enthalpy of hydrogenation [ΔH_{H2}(OL), Figure 3B] of the olefin compound examined (**I**), compared to reference compounds allyl anion (**G**) and ethylene (**H** in eq 4). The ΔH_{H2}(OL) value for allyl anion (**G**) is used to define equivalent conjugation (OL% = +100%), while ethylene (**G**) represents complete absence of conjugation (OL% = 0%), This olefinicity value is transformed to resonance enthalpy [H_{RE}(OL); eq 5].

$$\mathrm{OL\%} = m_{OL}\Delta H_{H2}(\mathrm{OL}) + b_{OL} \quad (4)$$

$$H_{RE}(\mathrm{OL}) = \mathrm{OL\%}/m_{OL} \quad (5)$$

Here, m_{OL} = 0.7441; b_{OL} = 98.4968 at B3LYP/cc-pVTZ in DMF.

Carbonylicity Percentage and Its Resonance Enthalpy (CA %). The "carbonylicity scale", quantifying carbonyl bond strength on a linear scale,[13] is based on the computed enthalpy of hydrogenation [ΔH_{H2}(CA), Figure 3C] of the compounds examined, compared to reference compounds, formate anion (**J**) and formaldehyde (**K**).[13] The ΔH_{H2}(CA) value for **J** is used to define perfect conjugation (eq 2; CA% = +100%), while **K** represents a complete absence of conjugation (CA% = 0%), defining a linear equation including m_{CA} and b_{CA} as linear parameters (eq 6). The carbonylicity value can be calculated by using eq 7, which may be transformed into resonance enthalpy [H_{RE}(CA)].

dx.doi.org/10.1021/jo300715d | J. Org. Chem. 2012, 77, 7282−7290

$$CA\% = m_{CA}\Delta H_{H2}(CA) + b_{CA} \quad (6)$$

$$H_{RE}(CA) = CA\%/m_{CA} \quad (7)$$

Here, m_{CA} = 0.5560 and b_{CA} = 45.2544 at B3LYP/cc-pVTZ in DMF.

■ ASSOCIATED CONTENT

Supporting Information

Definition of the concept of systems chemistry and detailed computational methods (Figure S1) and the concept of partitioning of compounds studied to their basic characteristics (Figures S2−S10, Tables S1−S4). Tables S5−S10 contain the computed energies, (E), zero-point energies (E_{ZPE}), internal energies (U), enthalpies (H), Gibbs free energies (G), and entropies (S) in hartrees at B3LYP/6-31G(d,p) and B3LYP/cc-pVTZ levels of theory. This material is available free of charge via the Internet at http://pubs.acs.org.

■ AUTHOR INFORMATION

Corresponding Author

*(Z.M.) Tel: +36-20-4416971. E-mail: zoltanmucsi@gmail.com. (B.V.) E-mail: volk.balazs@egis.hu.

Notes

The authors declare no competing financial interest.

■ DEDICATION

Dedicated to the memory of Professor István Hermecz.

■ REFERENCES

(1) Mucsi, Z.; Szabó, A.; Hermecz, I.; Kucsman, Á.; Csizmadia, I. G. *J. Am. Chem. Soc.* **2005**, *127*, 7615−7631.
(2) Buncel, E.; Stairs, R. A.; Wilson, H. In *The Role of the Solvent in Chemical Reactions*; Oxford University Press: Oxford, 2003.
(3) Ruff, F.; Csizmadia, I. G. In *Organic Reactions: Equilibria, Kinetics and Mechanism*; Elsevier: Amsterdam, 1994; Chapter 8, pp 232−239.
(4) Cramer, J. C. In *Essentials of Computational Chemistry*; John Wiley & Sons Ltd.: West Sussex, 2001; Chapter 7, p 433.
(5) Frank, E.; Mucsi, Z.; Zupkó, I.; Réthy, B.; Falkay, G.; Schneider, Gy.; Wölfling, J. *J. Am. Chem. Soc.* **2009**, *131*, 3894−3904.
(6) Mucsi, Z.; Viskolcz, B.; Csizmadia, I. G. *J. Phys. Chem. A* **2007**, *111*, 1123−1132.
(7) Mucsi, Z.; Körtvélyesi, T.; Viskolcz, B.; Csizmadia, I. G.; Novák, T.; Keglevich, G. *Eur. J. Org. Chem.* **2007**, 1759−1767.
(8) Mucsi, Z.; Viskolcz, B.; Hermecz, I.; Csizmadia, I. G.; Keglevich, G. *Tetrahedron* **2008**, *64*, 1868−1878.
(9) Mucsi, Z.; Csizmadia, I. G. *Curr. Org. Chem.* **2008**, *12*, 83−96.
(10) Mucsi, Z.; Tsai, A.; Szori, M.; Chass, G. A.; Viskolcz, B.; Csizmadia, I. G. *J. Phys. Chem. A.* **2007**, *111*, 13245−13254.
(11) Pilipecz, M.; Mucsi, Z.; Varga, T.; Scheiber, P.; Nemes, P. *Tetrahedron* **2008**, *64*, 5545−5550.
(12) Mucsi, Z.; Chass, G. A.; Viskolcz, B.; Csizmadia, I. G. *J. Phys. Chem. B.* **2008**, *112*, 7885−7893.
(13) Mucsi, Z.; Chass, G. A.; Viskolcz, B.; Csizmadia, I. G. *J. Phys. Chem. A.* **2008**, *112*, 9153−9165.
(14) Mucsi, Z.; Chass, G. A.; Viskolcz, B.; Csizmadia, I. G. *J. Phys. Chem. A.* **2009**, *113*, 7953−7962.
(15) Novák, T.; Mucsi, Z.; Blaskó, G.; Nyerges, M. *Synlett* **2010**, *16*, 2411−2414.
(16) Mucsi, Z.; Chass, G. A.; Csizmadia, I. G. *J. Phys. Chem. B* **2009**, *113*, 10308−10314.
(17) Mucsi, Z.; Ábrányi-Balogh, P.; Csizmadia, I. G. In *Energy Technology and Management: Energy managements in the chemical and biochemical world, as it may be understood from the Systems Chemistry point of view*; Aized, T., Ed.; InTech; 2011; Chapter 4, pp 79−110.
(18) Porcs-Makkay, M. *Simig. Gy. Org. Proc. Res. Dev.* **2000**, *4*, 10−16.
(19) Frisch, M. J.; Trucks, G. W.; Schlegel, H. B.; Scuseria, G. E.; Robb, M. A.; Cheeseman, J. R.; Zakrzewski, V. G.; Montgomery, J. A., Jr.; Stratmann, R. E.; Burant, J. C.; Dapprich, S.; Millam, J. M.; Daniels, A. D.; Kudin, K. N.; Strain, M. C.; Farkas, O.; Tomasi, J.; Barone, V.; Cossi, M.; Cammi, R.; Mennucci, B.; Pomelli, C.; Adamo, C.; Cliffordqq, S.; Ochterski, J.; Petersson, G. A.; Ayala, P. Y.; Cui, Q.; Morokuma, K.; Malick, D. K.; Rabuck, A. D.; Raghavachari, K.; Foresman, J. B.; Cioslowski, J.; Ortiz, J. V.; Baboul, A. G.; Stefanov, B. B.; Liu, G.; Liashenko, A.; Piskorz, P.; Komaromi, I.; Gomperts, R.; Martin, R. L.; Fox, D. J.; Keith, T.; Al-Laham, M. A.; Peng, C. Y.; Nanayakkara, A.; Challacombe, M.; Gill, P. M. W.; Johnson, B.; Chen, W.; Wong, M. W.; Andres, J. L.; Gonzalez, C.; Head-Gordon, M.; Replogle, E. S.; Pople, J. A. Gaussian 03 6.0, Gaussian, Inc., Pittsburgh PA, 2003.
(20) Beke, A. D. *J. Chem. Phys.* **1993**, *98*, 5648.
(21) Robonson, R. P.; Donahue, K. M. *J. Heterocycl. Chem.* **1994**, *31*, 1541−1544.